Electrochimica Acta 114 (2013) 838–843

Contents lists available at ScienceDirect

Electrochimica Acta

journal homepage: www.elsevier.com/locate/electacta

Surface characterisation of ASTM F139 stainless steel marked by laser and mechanical techniques

Eurico Felix Pieretti*, Isolda Costa[1]

Centro de Ciência e Tecnologia de Materiais, Instituto de Pesquisas Energéticas e Nucleares (CCTM-IPEN), Av. Prof. Lineu Prestes, 2242, São Paulo 05422-970, Brazil

ARTICLE INFO

Article history:
Received 5 February 2013
Received in revised form 27 May 2013
Accepted 27 May 2013
Available online 7 June 2013

Keywords:
Biomaterials
Corrosion
Surface characterisation
Stainless steel
Laser marks

ABSTRACT

The surfaces of implantable medical devices should present proper corrosion and mechanical resistance properties to fulfil their functions. Marking techniques are used for identification and traceability purposes but often generate surface modifications. Because surface defects affect corrosion resistance, the effects of marking processes must be investigated. This paper presents the effects of pulsed Nd:YAG laser marking techniques on the corrosion resistance of ASTM F139 austenitic stainless steel compared to that of mechanical marking techniques. The corrosion resistance was evaluated by electrochemical methods, and the surface was analysed by scanning electron microscopy with a field emission gun (SEM-FEG) coupled to an energy dispersive X-ray spectrometer. The surface characterisation showed the occurrence of microstructure variation due to the high temperatures involved in the laser melting process. Compared to the mechanical method, the laser marking technique had a deleterious effect on the resistance of ASTM F139 stainless steel to localised corrosion, increasing its susceptibility to pitting corrosion. These results were related to changes in the passive film properties, surface morphology and chemical composition.

1. Introduction

The use of materials in the human body is not a new idea [1]. Due to the observed increase in life expectancy, the number of related diseases in the elderly and the number of car accidents with irreversible injuries, advanced biomaterials continue to be researched and developed all around the world. Metallic biomaterials have found wide application in restorative surgery as basic materials for implantable medical devices for skeletal replacements and fixtures. For this purpose, metallic biomaterials that display great compatibility with biological environments, proper mechanical properties and high corrosion resistance are preferred [1–4].

Among metallic materials, ASTM F139 austenitic stainless steel has been employed for biomedical applications due to its mechanical properties, high corrosion resistance and moderately low cost. In general, stainless steels are largely applicable in medical implants such as orthopaedic replacements and stents due to their ease of fabrication and chemical stability [5]. All metallic biomaterials experience some electrochemical dissolution/corrosion in the area of the implant surrounded by the environment. The corrosion resistance of any implantable medical device is influenced by many factors, including the chemical composition, microstructure, pH, temperature, surface finishing and design [5,6].

Towards the end of the manufacturing process, marking techniques are often employed on metallic implantable medical devices for identification and traceability purposes and are performed according to the strictest standards of quality control.

Industrial marking techniques commonly used in Brazil include mechanical and laser methods. Compared to other methods, many advantages are associated with laser marking techniques, such as high degree of automation, great reproducibility of characters, quickness and cleanliness [7,8]. Moreover, the laser process produces less surface distortion and produces high quality, durable and well-defined inscriptions [9]. Laser marking techniques can be used for various applications such as cutting, welding, ablation, hardening and engraving and to create decorative textures [10–12]. However, the effect of laser marking techniques on the surface corrosion resistance has not yet been intensely investigated.

The aim of the present work was to evaluate the effect of laser and mechanical marking techniques on the susceptibility of ASTM F139 stainless steel to localised corrosion.

2. Experimental

The material used in the current study was ASTM F139 austenitic stainless steel. The composition of the steel was determined by optical emission spectroscopy and is shown in Table 1. ASTM

* Corresponding author. Tel.: +55 11 3133 9226.
E-mail addresses: efpieretti@usp.br, e_pieretti@terra.com.br (E.F. Pieretti).
[1] Tel.: +55 11 3133 9226.

0013-4686/$ – see front matter © 2013 Elsevier Ltd. All rights reserved.
http://dx.doi.org/10.1016/j.electacta.2013.05.101

Table 1
Chemical composition of the ASTM F139 stainless steel.

Element	C	Si	Mn	P	S	Cr	Mo	Ni	Fe
(wt.%)	0.023	0.378	2.09	0.026	0.0003	18.32	2.59	14.33	Balance

F139 austenitic stainless steel is largely used for the fabrication of orthopaedic implants. Two types of marking techniques were used, including a mechanical and laser method. Samples without marks were also tested for comparative purposes. For these experiments, a pulsed Nd:YAG laser was operated at a wavelength of 1064 nm, a frequency of 20 Hz and a scanning speed of 4 mm s^{-1}. The procedure consisted of marking the number 8 (eight) on the surface of the samples many times in order to modify a large area of the sample, which caused the overlapping of passes at the centre of the marked number with the laser beam. The mechanical method consisted of engraving the surface via plastic deformation, which removed the material.

The corrosion resistance tests were carried out using electrochemical techniques, including electrochemical impedance spectroscopy (EIS) and potentiodynamic polarisation. All of the electrochemical tests were carried out using a three-electrode cell set-up with a Pt counter electrode (wire with a geometric area of 2.0 cm^2) and an Ag/AgCl reference electrode (3 M). The area of the working electrode exposed to the electrolyte was 1 cm^2. To evaluate the reproducibility of the results, four samples were tested for each surface condition. The electrolyte consisted of a phosphate-buffered saline (PBS) solution with a pH of 7.4. The chemical composition of the electrolyte is shown in Table 2. The solution was prepared from high purity reagents and deionised water. The polarisation tests were performed at a scan rate of 0.167 mV s^{-1} and a temperature of (37 ± 1)°C, after monitoring the open circuit potential (OCP) for 17 h. All of the electrochemical experiments were carried out using Gamry PCI4/300 equipment

Surface characterisation was conducted using a scanning electron microscope coupled to a high-resolution field emission gun (SEM-FEG, FEI – INSPECT F50).

3. Results and discussion

3.1. Open circuit potential measurements

Fig. 1 shows the open circuit potential (OCP) as a function of the immersion time for the various types of surfaces during a period of 17 h of immersion in PBS solution. The observed variation in the OCP over time indicated the laser-marked sample's susceptibility to pitting, as evidenced in the first period of immersion, which showed frequent drops followed by an exponential increase in the potential. This period was followed by a continuous and slow drop in potential between 2×10^4 and 4×10^4 s of immersion, likely due to the generalised attack of the passive film. The observed decrease in potential may be associated with the etching and removal of the weakest areas of the oxide layer. After this period, a slow potential increase occurred, which was indicative of the thickening or formation of a more homogeneous oxide surface film after the removal of defective areas. For the laser-marked samples, the samples marked by laser technique potential stabilisation in the was only reached after approximately 15 h of immersion, which indicated that the passive film presented a high degree of unevenness on the surface of laser-marked samples. From the first period until 16 h of immersion, the potential variation of samples with laser marks was approximately 0.3 V.

For unmarked or mechanically marked samples, the potential was more stable from the beginning of the immersion period. All of the samples reached reasonable stabilisation after 10 h of immersion. For samples with marks made mechanically, the potential showed a slow decrease until stabilisation occurred, which was indicative of the slight attack of the passive film. Defective areas around the marks were likely regions where the oxide was preferentially attacked. For the unmarked surface, the potential shifted to a slightly more noble direction over time due to oxide film growth.

Table 2
Chemical composition of phosphate buffered saline (PBS) solution (pH 7.4).

Compound	Concentration (g/L)
NaCl	8.0
KCl	0.2
Na_2HPO_4	1.15
KH_2PO_4	0.2

3.2. EIS measurements

The Bode plots (phase angle) in Fig. 2(a) show phase angles between −70° and −80° at a large range of frequencies. High angles at low frequencies are typical of passive materials. For unmarked or mechanically marked samples, the plateau ranged from 10 Hz to 10^{-2} Hz, whereas high angles began at frequencies of 1 Hz for laser-marked samples. In the literature, this behaviour is associated with stainless steels containing a passive oxide film [14,16]. The electrochemical phenomena at the oxide film–electrolyte interface were related to the medium frequency response, whereas those at the substrate–oxide interface were associated with the low frequency results [13–17]. The interaction of these two types of electrochemical phenomena is responsible for the observed plateau. The Bode (*Z* modulus) diagrams presented in Fig. 2(b) showed that the lowest impedances were associated with laser-marked samples and the highest impedances corresponded to unmarked samples, indicating that the laser-marked samples displayed the lowest corrosion resistance.

The experimental EIS data were adjusted to two equivalent electric circuits (EECs), depending on the type of surface tested, as illustrated in Fig. 3. The models were proposed to simulate the electrochemical behaviour of the substrate–oxide and oxide–electrolyte interfaces. These models have been widely used

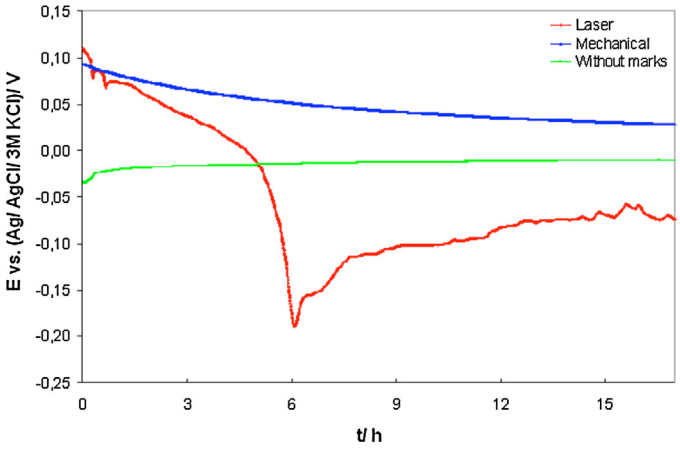

Fig. 1. Open circuit potential variation with time of immersion for unmarked, laser marked and mechanically marked surfaces during 17 h of immersion in phosphate buffer saline solution at 37 °C.

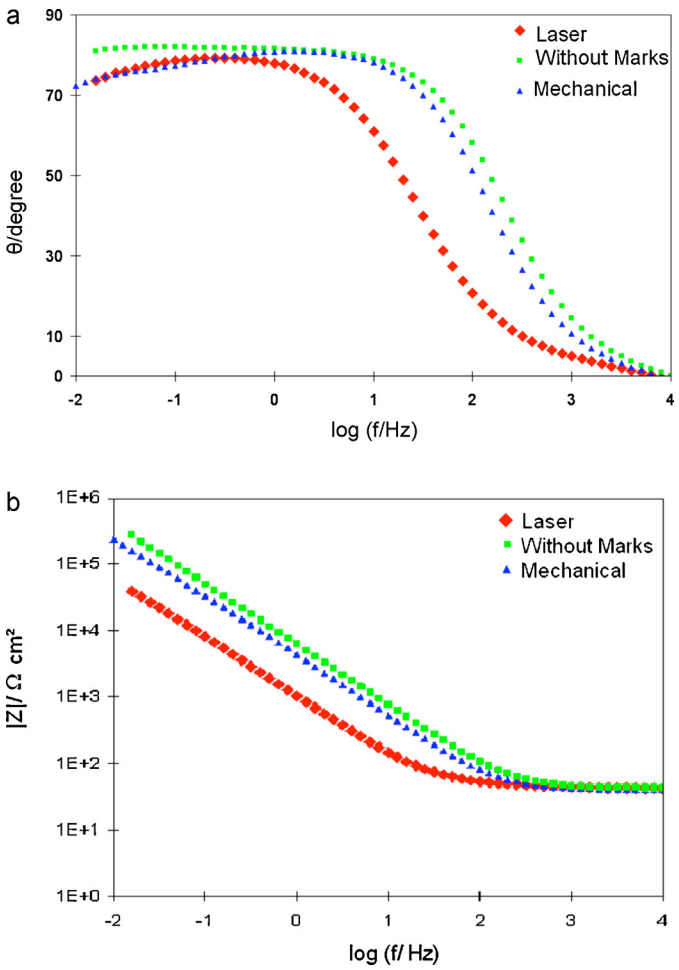

Fig. 2. (a) Bode phase angle, (b) Bode *Z* modulus diagrams for ASTM F139 stainless steel samples with unmarked, mechanically or laser marked surfaces.

in the literature to simulate the electrochemical behaviour of passive stainless steel. Passive films formed on stainless steels show dichotomous character, having an inner chromium-rich oxide region and an outer iron-rich oxide and hydroxide region [18–21]. In the EECs proposed in the present study, CPE are constant phase elements, C is an ideal capacitor and R represents the resistance at the interfaces. In the published literature [22–24], the response at high frequencies has been proposed. In the present work, the R2/CPE2 pair was associated with the oxide film–electrolyte interface, whereas the R3/CPE3 pair or R3/C3 pair, which

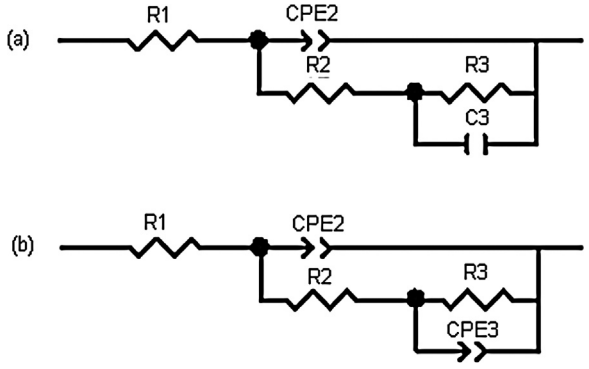

Fig. 3. Equivalent electrical circuits proposed to adjust the experimental data of electrochemical impedance spectroscopy test to characterise the passive film on (a) samples marked by laser and without marks, (b) mechanically marked samples.

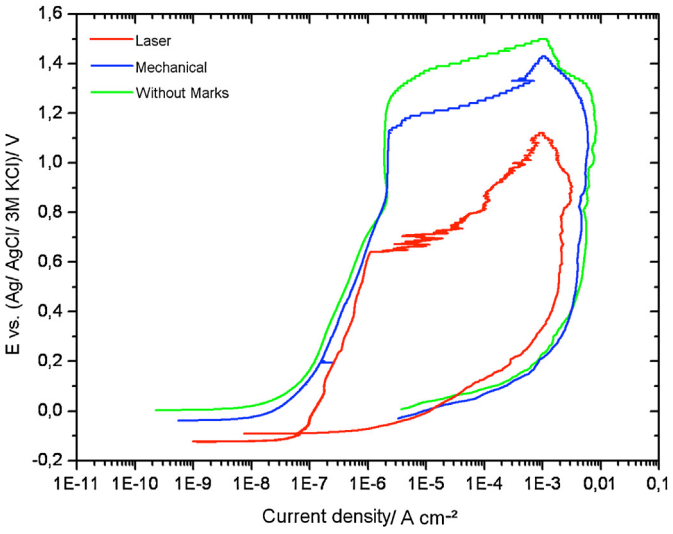

Fig. 4. Cyclic polarisation curves typical of the electrochemical behaviour of the three types of surface tested. Results obtained in phosphate buffer saline solution at 37 °C after 17 h of immersion (scan rate: 0.167 mV s^{-1}).

corresponded to the response at lower frequencies, was related to the substrate–oxide film interface.

The values obtained for the EEC components are shown in Table 3. As shown in the table, significantly lower R2 values were associated with laser-marked samples. This resistance was related to charge transfer at the oxide film–electrolyte interface and was much lower than those of the other types of tested surfaces.

The low R2 values, which were on the order of those related to the electrolyte (R1), may be indicative of the formation of a porous oxide/hydroxide layer containing pores filled with the electrolyte. In addition, the n2 values, which indicated that the outer part of the oxide layer (oxide–electrolyte interface) was heterogeneous, suggested that laser-marked samples possessed a more uneven surface. The highest CPE2 values were associated with the surface of laser-marked samples, which was indicative of a more reactive interface. Moreover, the R3 values, which were 10 times greater for unmarked or mechanically marked samples than those of laser-marked samples, showed that the inner substrate–oxide film interface of the unmarked surface was also less resistant to corrosion.

The inner region of the oxide film was related to a chromium-rich layer. Compared to the other samples, the relatively large differences in laser-marked samples suggested that the chemical composition was affected by the laser marking process.

3.3. *Cyclic polarisation curves*

The cyclic potentiodynamic polarisation curves shown in Fig. 4 also supported the previously presented electrochemical results. The pitting potential of samples with laser marks were well below those observed for unmarked or mechanically marked samples, showing the greater susceptibility of laser-affected areas to pitting. The pitting susceptibility of the samples was also evidenced by the current oscillations observed prior to the breakdown of the passive film.

The large hysteresis observed in the curves for the three conditions indicated that pits formed in all three types of surfaces, and the tendency for repassivation in the test medium was low.

The results indicated that the oxide that formed on laser-marked surfaces had a greater number of defects than those produced under the other tested conditions.

Table 3
Values obtained from fitting for the components of the equivalent electrical circuits shown in Fig. 3.

	R1 ($\Omega\,cm^2$)	CPE2 ($cm^{-2}\,s^{-n}\,\Omega$)	n2	R2 ($\Omega\,cm^2$)	CPE3 ($cm^{-2}\,s^{-n}\,\Omega$)	n3	C3 ($cm^{-2}\,s^{-n}\,\Omega$)	R3 ($\Omega\,cm^2$)
Without marks	44.23	2.8×10^{-5}	0.921	1.7×10^{5}	–	–	2.2×10^{-6}	6.8×10^{6}
Laser	42.84	1.5×10^{-4}	0.861	81.36	–	–	3.4×10^{-5}	4.2×10^{5}
Mechanical	41.62	4.2×10^{-5}	0.917	2.1×10^{5}	8.8×10^{-6}	0.796	–	1.8×10^{6}

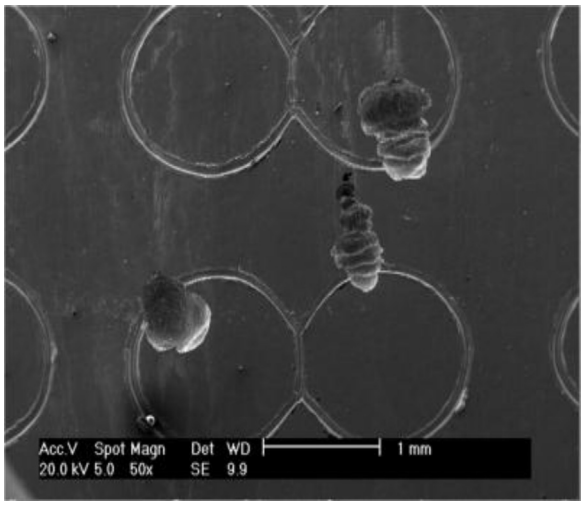

Fig. 5. ASTM F139 SS mechanically marked surface, after anodic polarisation test in phosphate buffer saline solution at 37 °C.

The SEM-FEG micrographs of the surface reinforced the aforementioned results, as shown in Figs. 5 and 6.

The observed defects were due to thermal effects caused by the laser, which melted the material [7–12], leading to changes in the surface topography and defects such as dislocations associated with strain. In fact, a large number of dislocations were observed, as evidenced by etch pits in areas between the molten zone (marked area) and the stainless steel matrix, as shown in Fig. 7. These defects may form peaks and valleys, creating occluded areas that act as crevices and favour localised attack.

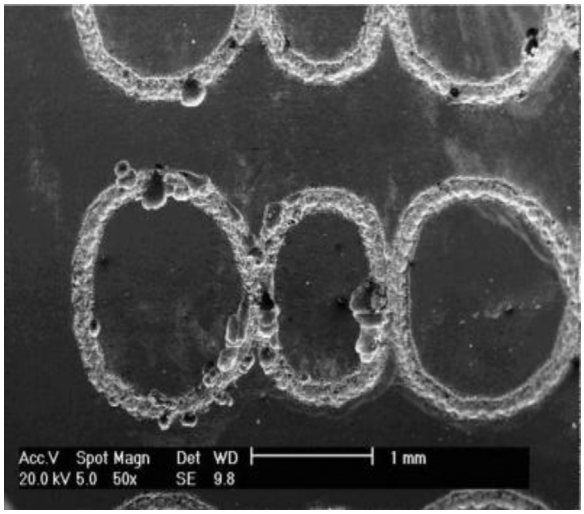

Fig. 6. ASTM F139 SS marked by laser, after anodic polarisation test in phosphate buffer saline solution at 37 °C.

3.4. Surface finishing analyses

Figs. 5 and 6 show the surface of stainless steel marked mechanically or with a laser after the cyclic polarisation tests, respectively. The laser marking process changed the characteristics of the passive film and contributed to the observed decrease in the resistance of the biomaterial to localised corrosion.

The effects of the laser marking techniques included increased roughness due to the melting of the surface and the interface between the molten zone and the matrix, which possessed a high dislocation density, as evidenced by etch pits [25,26]. To evaluate these effects on the samples, SEM images were obtained after marking and prior to electrochemical testing, as shown in Fig. 7(a) and (b).

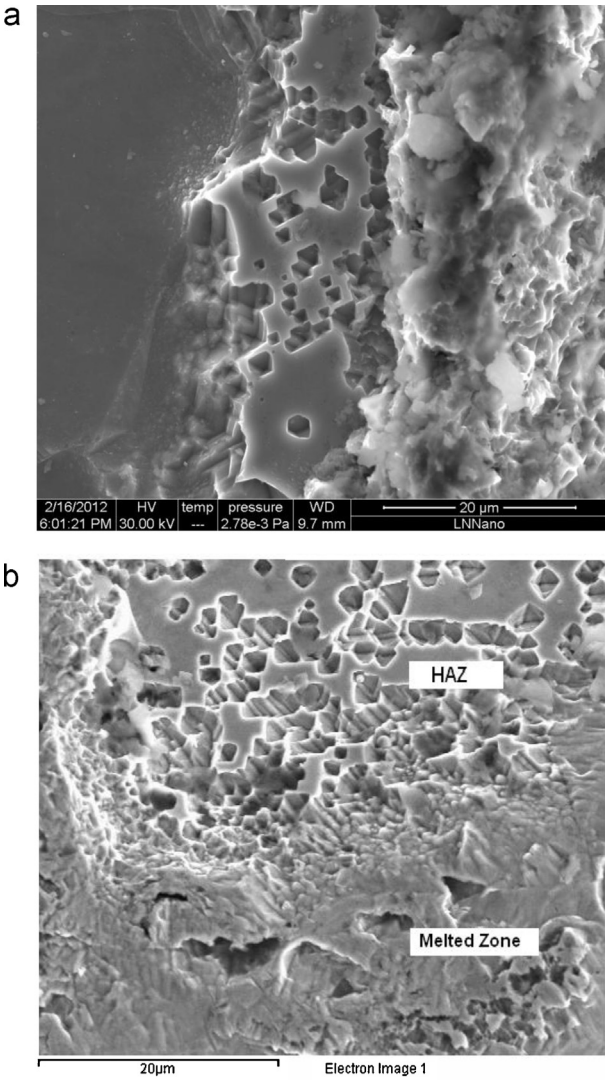

Fig. 7. Micrographs of the ASTM F139 SS surface, marked by laser, prior to polarisation tests. (a) The matrix (left side), etch pits area between the matrix and the melted zone, and (b) etch pits and melted zone. The etch pits indicate a high density of dislocations at the heat affected zone.

Table 4
EDX semiquantitative chemical composition (wt. %) of the areas presented in Fig. 8.

Element	(a)	(b)	(c)
Si	0.4	1.3	0.6
Cr	18.3	25.2	30.0
Mn	1.9	4.3	6.1
Fe	61.5	54.8	53.8
Ni	14.5	11.2	6.8
Mo	3.4	3.1	2.6

An important effect of the laser marking technique was the significant change in the surface chemical composition, as shown in Table 4, which displays data obtained by semi-quantitative analysis of the EDX spectra of different regions of the samples prior to cyclic polarisation (Fig. 8). Three areas were investigated: (a) the matrix, i.e., the base material without any marks, (b) marked areas where the laser beam was focused once and (c) marked areas where the laser was focused twice at the centre of the number eight. The laser marking technique did not remove any of the material but melted the surface. EDX data were indicative of Cr enrichment and Mo impoverishment in the laser-marked area. Laser pulses are rapid and extremely localised, and Cr does not evaporate. This element concentrates in an area and impoverishes surrounding regions. Thus, corrosion occurred at areas adjacent to the site of laser marking.

Mahmoudi et al. investigated the influence of a pulsed Nd:YAG laser on the surface hardness of a martensitic stainless steel and observed an increase in Cr on samples treated with a laser compared to unmarked samples. In addition, pulse overlapping significantly decreased the pitting potential of the material [27].

The effects of Mo on stainless steels are well known [28,29]. The addition of Mo to austenitic stainless steels increases the localised corrosion resistance, mainly in chloride containing environments reducing anodic dissolution rate. Mo adsorbs to weaker areas of the surface, and its effect is related to the formation of molybdates, which increase the resistance of the oxide film. Mn is added to steel to limit the deleterious effects of sulphur. Specifically, Mn addition leads to the formation of MnS, which decreases the amount of S available to combine with Fe. FeS is more electrically conductive than MnS, favouring the formation of microcells [28,30]. Mn might also be added to increase the solubility of nitrogen [31].

Jang and Kwon studied the effects of Ni and Mo on the passive film formed on Fe–20Cr alloys. They observed that by alloying with Ni, the corrosion potential of the Fe–20Cr alloy was raised in the noble direction, and by alloying with Mo, the passive current density was decreased comparatively to the Fe–20Cr alloy. Photoelectrochemical and Mott–Shottky techniques confirmed that the passive films formed on Fe–20Cr alloys have a structure of Cr-substituted γ-Fe_2O_3 with variation of donors densities depending on the Ni and Mo contents in the alloy [32].

Molybdenum has been found to be beneficial to stainless steels, especially under active corrosion conditions, such as the chemical environment of blood plasma [6]. Mo also increases the stability of Fe^{3+} in the passive film, at polymerised insoluble molybdates films, in the form of $Fe_2(MoO_4)_3$ [33].

Some authors proposed that Mo acted by forming a protective film of MoO_2 or a comparable hydrated oxide, since Mo remained passive at lower pH values than other alloying elements of stainless steels [34]. Other authors associated the enrichment of Cr in the oxide layer to the selective dissolution of Mo [35,36].

Pardo et al. [37] investigated the effect of Mo and Mn additions on the corrosion resistance of two austenitic stainless steels, AISI 304 and 316, in 30 wt.% H_2SO_4. They observed that additions of 2.7 wt.% of Mo practically inhibited the corrosion process at 25 °C, and the Mn addition did not appreciably affect the corrosion resistance. Furthermore, Mo addition shifted the corrosion potential to

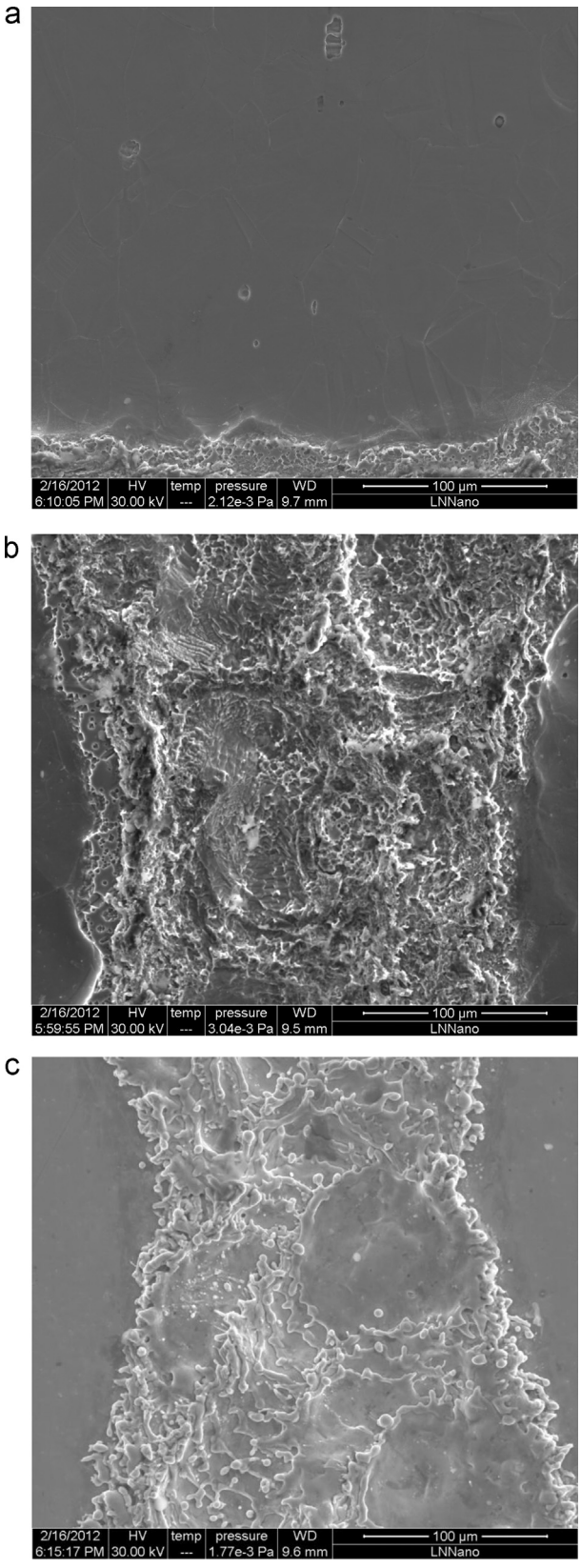

Fig. 8. Micrographs of the ASTM F139 SS, prior to electrochemical tests. (a) Region without laser marks, (b) rough areas due to laser marking process (one pass) and (c) defects at the laser marked areas (overlapping of passes).

more noble values and reduced the current density in the active region. The authors concluded that the decreased corrosion susceptibility of the steels by molybdenum addition in sulphuric acid media may be attributed to the formation of an insoluble and protective MoO_3 layer [37].

4. Conclusions

The studied laser marking technique had a deleterious effect on the resistance of ASTM F139 stainless steel to localised corrosion, increasing its susceptibility to pitting corrosion compared to that of the mechanical method, as evidenced by all of the results obtained in the present study.

The EIS results indicated that the laser marking process largely decreased the resistance of the metallic substrate–oxide film and oxide–electrolyte interfaces, favouring localised attack. The laser process created a region with a high density of dislocations between the molten zone and steel matrix, as indicated by the formation of etch pits. Moreover, chromium enrichment and nickel and molybdenum impoverishing occurred at areas affected by the laser beam, as shown in the EDX analysis.

Acknowledgements

The authors thank the Instituto de Ortopedia e Traumatologia do Hospital das Clínicas da Faculdade de Medicina da Universidade de São Paulo (IOT-HCFMUSP) and the Laboratório Nacional de Nanotecnologia (LNNano).

References

[1] D.J. Lyman, W.J. Seare Jr., Biomedical materials in surgery, Materials Science 4 (1974) 415.
[2] D.F. Williams, Corrosion of implant materials, Materials Science 6 (1976) 237.
[3] D.F. Gibbons, Biomedical materials, Biophysics and Bioengineering 4 (1975) 367.
[4] L.L. Hench, Prosthetic implant materials, Materials Science 5 (1975) 279.
[5] Y.C. Tang, S. Katsuma, S. Fujimoto, S. Hiromoto, Electrochemical study of type 304 and 316 L stainless steel in simulated body fluids and cell cultures, Acta Biomaterialia 2 (2006) 709.
[6] S. Virtanen, I. Milošev, E. Gomez-Barrena, R. Trebše, J. Salo, Y.T. Konttinen, Special modes of corrosion under physiological and simulated physiological conditions, Acta Biomaterialia 4 (2008) 468.
[7] C. Leone, S. Genna, G. Caprino, I. De Iorio, AISI 304 stainless steel marking by a Q-switched diode pumped Nd:YAG laser, Journal of Materials Processing Technology 210 (2010) 1297.
[8] J. Qi, K.L. Wang, Y.M. Zhu, A study on the laser marking process of stainless steel, Journal of Materials Processing Technology 139 (2003) 273.
[9] F.J. Gil, L. Delgado, E. Espinar, J.M. Llamas, Corrosion and corrosion-fatigue behavior of cp–Ti and Ti–6Al–4V laser-marked biomaterials, Journal of Materials Science: Materials in Medicine 23 (2012) 885.
[10] L. Costa, K. Lansford, D. Rajput, W. Hofmeister, Unique corrosion and wear resistant identification tags via LISI™ laser marking, Surface & Coatings Technology 203 (2009) 1984.
[11] J. Diaci, D. Bračun, A. Gorkič, J. Možina, Rapid and flexible laser marking and engraving of tilted and curved surfaces, Optics and Lasers in Engineering 49 (2011) 195.
[12] M.E. Jazi, M.D. Baghi, M. Hajimahmodzadeh, M. Soltanolkotabi, Pulsed Nd:YAG passive Q-switched laser using Cr^{4+}:YAG crystal, Optics and Laser Technology 44 (2012) 522.
[13] C. Liu, Q. Bi, A. Leyland, A. Matthews, An electrochemical impedance spectroscopy study of the corrosion behavior of PVD coated steels in 0.5 N NaCl aqueous solution, Part I, Corrosion Science 45 (2003) 1243.
[14] K.R. Trethewey, M. Paton, Electrochemical impedance behaviour of type 304 L stainless steel under tensile loading, Materials Letters 58 (2004) 3381.
[15] S. Krakowiak, K. Darowicki, P. Slepski, Impedance investigation of passive 304 stainless steel in the pit pre-initiation state, Electrochimica Acta 50 (2005) 2699.
[16] J. Ji, Q. Tan, D. Fan, F. Sun, M.A. Barbosa, J. Shen, Fabrication of alternating polycation and albumin multilayer coating onto stainless steel by electrostatic layer-by-layer adsorption, Colloids and Surfaces B: Biointerfaces 34 (2004) 185.
[17] V.A. Alves, R.Q. Reis, I.C.B. Santos, D.G. Souza, T. Gonçalves, M.A. Pereira, A. Rossi, L.A. Silva, In situ impedance spectroscopy study of the electrochemical corrosion of Ti and Ti–6Al–4V in simulated body fluid at 25 °C and 37 °C, Corrosion Science 51 (2009) 2473.
[18] N.E. Hakiki, M.F. Montemor, M.G.S. Ferreira, M. Da Cunha Belo, Semiconducting properties of thermally grown oxide films on AISI 304 stainless steel, Corrosion Science 42 (2000) 687.
[19] M. Da Cunha Belo, N.E. Hakiki, M.G.S Ferreira, Semiconducting properties of passive films formed on nickel-base alloys type Alloy 600: influence of the alloying elements, Electrochimica Acta 44 (1999) 2473.
[20] L.V. Taveira, M.F. Montemor, M. Da Cunha Belo, M.G. Ferreira, L.F.P. Dick, Influence of incorporated Mo and Nb on the Mott–Schottky behaviour of anodic films formed on AISI 304 L, Corrosion Science 52 (2010) 2813.
[21] N.E. Hakiki, S. Boudin, B. Rondot, M. Da Cunha Belo, The electronic structure of passive films formed on stainless steels, Corrosion Science 37 (1995) 1809.
[22] K. Azumi, T. Ohtsuka, N. Sato, Impedance of iron electrode passivated in borate and phosphate solutions, Transactions of the Japan Institute of Metals 27 (1986) 382.
[23] H. Ge, G. Zhou, W. Wu, Passivation model of 316 stainless steel in simulated cooling water and the effect of sulfide on the passive film, Applied Surface Science 211 (2003) 321.
[24] H. Gerischer, Models for the discussion of the photo-electrochemical response of oxide layers on metals, Corrosion Science 29 (1989) 257.
[25] Y. Yang, Y. Lu, J. Wang, Y. Dai, B. Sun, Distribution of dislocation etch pits and its influence on the optical properties of 2 μm waveband Tm:YAP laser crystal, Journal of Alloys and Compounds 455 (2008) 1.
[26] H.O. Santos, N.B. Lima, V.A. Rodrigues, J.L. Rossi, W.A. Monteiro, Scanning electron microscopic evaluation of etch pitted Fe–3%Si specimens, Acta Microscopica 9 (2000) 309.
[27] B. Mahmoudi, M.J. Torkamany, A.R. Sabour Routh Aghdam, J. Sabbaghzade, Laser surface hardening of AISI 420 stainless steel treated by pulsed Nd:YAG laser, Materials and Design 31 (2010) 2553.
[28] A. Szummer, M. Janik-Czachor, Corrosion behaviour of low-manganese stainless steel, Corrosion Science 35 (1993) 317.
[29] J.L. Polo, E. Cano, J.M. Bastidas, An impedance study on the influence of molybdenum in stainless steel pitting corrosion, Journal of Electroanalytical Chemistry 537 (2002) 183.
[30] D.E. Williams, M.R. Kilburn, J. Cliff, G.I.N. Waterhouse, Composition changes around sulphide inclusions in stainless steels, and implications for the initiation of pitting corrosion, Corrosion Science 52 (2010) 3702.
[31] R.F.A. Jargelius-Pettersson, Application of the pitting resistance equivalent concept to some highly alloyed austenitic stainless steel, Corrosion 54 (1998) 162.
[32] H. Jang, H. Kwon, In situ study on the effects of Ni and Mo on the passive film formed on Fe–20Cr alloys by photoelectrochemical and Mott–Schottky techniques, Journal of Electroanalytical Chemistry 590 (2006) 120.
[33] Z. Feng, X. Cheng, C. Dong, L. Xu, X. Li, Passivity of 316 L stainless steel in borate buffer solution studied by Mott–Schottky analysis, atomic absorption spectrometry and X-ray photoelectron spectroscopy, Corrosion Science 52 (2010) 3646.
[34] W. Yang, R.C. Ni, H.Z. Hua, A. Pourbaix, The behaviour of chromium and molybdenum in the propagation process of localized corrosion of steels, Corrosion Science 24 (1984) 691.
[35] K. Hashimoto, K. Asami, A. Kawashima, H. Habazaki, E. Akiyama, The role of corrosion-resistant alloying elements in passivity, Corrosion Science 49 (2007) 42.
[36] M.W. Tan, E. Akiyama, A. Kawashima, K. Asami, K. Hashimoto, The effect of air exposure on the corrosion behaviour of amorphous Fe–8Cr–Mo–13P–7C alloys in 1 M HCl, Corrosion Science 37 (1995) 1289.
[37] A. Pardo, M.C. Merino, A.E. Coy, F. Viejo, R. Arrabal, E. Matykina, Effect of Mo and Mn additions on the corrosion behaviour of AISI 304 and 316 stainless steels in H_2SO_4, Corrosion Science 50 (2008) 780.